Free Radical Formation in Supercritical CO_2, Using Muonium as a Probe and Implication for H Atom Reaction with Ethene

P. Cormier,[†] D. J. Arseneau,[‡] J. C. Brodovitch,[§] J. M. Lauzon,[†] B. A. Taylor,[†] and K. Ghandi*,[†]

Department of Chemistry, Mount Allison University, Sackville, New Brunswick, E4L 1G8, Canada; TRIUMF, Vancouver, British Columbia, Canada; Department of Chemistry, Simon Fraser University, Burnaby, British Columbia, V5A 1S6, Canada

Received: February 3, 2008; Revised Manuscript Received: March 3, 2008

This report presents the first observation of an alkyl radical in supercritical CO_2 by any magnetic resonance technique. Muoniated ethyl radical has been detected in muon-irradiated supercritical CO_2 solutions. In the presence of a low concentration of ethene in supercritical CO_2, it is found that the addition of muonium to ethene is the only reaction channel, and that the yield of this process is enhanced compared to conventional solvents. The temperature dependence of the hyperfine coupling constants of the ethyl radical suggests that at a density of 0.3 g/cm^3 both the rotational motion of the methyl group and the electronic structure of the radical are similar to those in the gas phase, and therefore that the local environment around the ethyl radical is similar to the gas phase under these conditions. At higher densities, however, there is a remarkable and unexpected density dependence of the hyperfine coupling constant of the ethyl radical, which has never been observed in any environment. In this regime, the density dependence suggests that supercritical CO_2 has a significant effect on the electronic structure of the free radical. Thus, changing the density of CO_2 offers a possible means of tuning the radical reactivity. In addition, at a density of close to 0.4 g/cm^3, CO_2 molecules cluster around the ethyl radical, and this increases the local density around the ethyl radical by a factor of ∼1.5.

1. Introduction

The role of the solvent in chemical reactions is multifaceted; for instance, the choice of solvent can alter the rate of reactions, and thus determine the pathway and the product yield in chemical synthesis.[1] Supercritical CO_2 ($scCO_2$) has been found to be a useful "green" solvent for a wide variety of chemical applications,[2] including free radical polymerization[1,3,4] and photochemical reactions.[5–8] Carbon dioxide is inexpensive, is nonflammable, and has a readily accessible supercritical region (P_c = 7.38 MPa, T_c = 304.15 K) allowing a wider range of control of reaction conditions. It is an energy-conserving, selective, and waste-reducing alternative to organic solvents. Moreover, the use of $scCO_2$does not add to the greenhouse effect as it can easily be conserved during industrial processes.[1,3,4]

In supercritical fluids, the solvent properties (density, dielectric constant, etc.) vary with the temperature and pressure. Because of their easily tunable properties between those of liquids and gases, supercritical fluids and in particular $scCO_2$ provide reaction-oriented media for chemical processes.[1,4,5] The change in the solvent properties could significantly affect the electronic structures of the reactive intermediates and the corresponding transition states. In this context, free radicals are often invoked to explain the mechanism of the reactions,[5–7] and observation of such intermediate species is essential to establish their involvement in $scCO_2$.

Most free radical mechanistic information in $scCO_2$ is based on product analysis.[1,3,4,8–10] Very little information exists on reactive (nonpersistent) organic radicals in $scCO_2$.[11,12] This is surprising since characterization of neutral free radicals in a wide range of thermodynamic conditions in $scCO_2$ would have a huge impact on free radical polymerization.[9,10,12]

Recently transient absorption spectroscopy in supercritical CO_2[13–15] has provided information on the dynamics of the reactive intermediates. When such intermediate species are indeed observable, measurements of hyperfine coupling constants (hfc's) are sensitive probes of the electronic structures of these radical intermediates allowing an examination of the effect of solvent interactions on their electronic structures.[16] Extraction of information on the electronic structure and hyperfine interactions in neutral free radicals by absorption spectroscopy is very difficult. Electron spin resonance (ESR) can detect radicals generated from the radiation processes and provide nuclear hyperfine coupling constants, but it is limited in its ability to probe reactive free radicals such as the ethyl radical in supercritical CO_2.[11] The construction of the fast 9.5 GHz time-resolved electron paramagnetic resonance spectrometer (TREPR) with a high-pressure probe by Avdievich[17] and Forbes[18] has been an important step forward. This technique has recently been used to study initiator addition to methyl methacrylate in liquid and $scCO_2$.[12] Such studies are very important as they provide information on the addition of a free radical to an alkene, a process which is always present in free radical polymer synthesis. The TREPR studies[12] are usually performed at very high concentrations such that the monomers could perturb the critical properties of CO_2. Hence, it may be difficult to attribute changes in the hyperfine interactions to solute−solvent interactions. Also, some free radicals cannot be distinguished from each other by TREPR under supercritical conditions.[12] Another difficulty is the fast spin relaxation compared to the time resolutions of TREPR spectroscopy.[12] Such problems can make TREPR studies of small and simple

* Corresponding author. E-mail: kghandi@mta.ca.
† Mount Allison University.
‡ TRIUMF.
§ Simon Fraser University.

10.1021/jp801023v CCC: $40.75
Published on Web 04/23/2008

SCHEME 1: Reaction of the Hydrogen Atom Surrogate Muonium with Ethene To Produce the Muon-Substituted Ethyl Radical

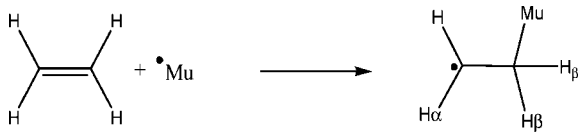

free radicals such as ethyl radical in supercritical CO_2 very difficult. The present study, as explained later, can provide both unique and complementary information to TREPR spectroscopy.

The simplest neutral free radical is the hydrogen atom, and therefore studying its reactions with simple alkenes will provide important fundamental information on free radical formation in $scCO_2$. In the condensed phase, the hydrogen atom is usually produced through radiolysis of protonated compounds. Therefore, in pure $scCO_2$, H atom is impossible to generate in this way. Muonium (Mu = $[\mu^+e^-]$, ~0.11 amu) is closely related to the hydrogen atom. It is a hydrogen-like atom which has the muon, μ^+, as its nucleus.[19,20] The reduced mass and ionization potential of H and Mu are almost identical, which means that their electronic properties are almost the same. In this context, Mu can be considered a light isotope of H. In addition, the muon has a magnetic moment ca. 3.2 times that of the proton, and muon beams can be produced 100% spin polarized. Therefore, the suite of spectroscopic methods broadly called muon spin resonance (μSR) are much more sensitive than EPR.[19,20] The only report using muons in supercritical CO_2 is the work of Ghandi et al.,[21] where muonium formation in supercritical CO_2 was investigated.

In conventional solvents, reactions of Mu with unsaturated molecules occur rapidly to generate muoniated free radicals which can be detected using μSR. The present work reports probing the reaction of H atom with ethene using muonium and reports the first detection of a muoniated free radical in supercritical CO_2 (see Scheme 1).

The ethyl radical is often considered to be a benchmark for both theoretical calculations and experiments because its small size allows for extensive calculations that can include vibrational averaging.[22–26] Experimental studies of the ethyl radical by ESR even in the gas phase at standard conditions are difficult due to its high reactivity, spin relaxation (short lifetime) and the complications of its production.[27] Here, we report the formation of the $C_2H_4Mu^•$ radical in $scCO_2$and the corresponding muon and proton hyperfine interactions and compare the results to those previously obtained in pure ethene in the gas phase.[22–26]

The purpose of the present study is to answer the following questions:

(a) Would a Mu (or H) atom react with a dilute solution of ethene in supercritical CO_2, or would ethene modify the solvent properties of CO_2 (as a cosolvent) and promote reaction of either Mu or Mu* (Mu before thermalization) with the more abundant CO_2 molecules?

(b) Would supercritical CO_2 at higher densities react with alkyl radicals?

(c) CO_2 molecules have large quadrupole moments. Would such a large quadrupole moment lead to a considerable interaction of CO_2 molecules and alkyl radicals to affect the hfc's of the alkyl radicals in supercritical CO_2?

(d) Do such interactions depend on the pressure (density)?

(e) What is the effect of CO_2 molecules on the distribution of unpaired electron density of a simple alkyl radical (and electron density in general)?

2. Experimental Section

Experiments were carried out on the M9B high momentum muon channel of the TRIUMF cyclotron facility, in Vancouver, Canada, using muon spin spectroscopic techniques.

In μSR the spectroscopic information is carried by the positrons emitted during the decay of the muon in the muoniated species. These positrons are detected by plastic scintillators located outside the sample cell. Figure 1 shows the schematic of our setup. The heated pressure cell (high pressure target cell in Fig. 1) and associated plumbing are supported inside a water-cooled jacket and shield. This shield protects the surrounding heat-sensitive plastic scintillators and light guides of the positron detectors, which transfer the light to photomultiplier tubes (PMT in Figure 1), from the heat generated by the heater surrounding the high-pressure cell.

A beam of spin-polarized positive muons (~75 MeV/c) was allowed to stop in the sample contained in a pressure vessel mounted in the HELIOS μSR spectrometer (superconducting

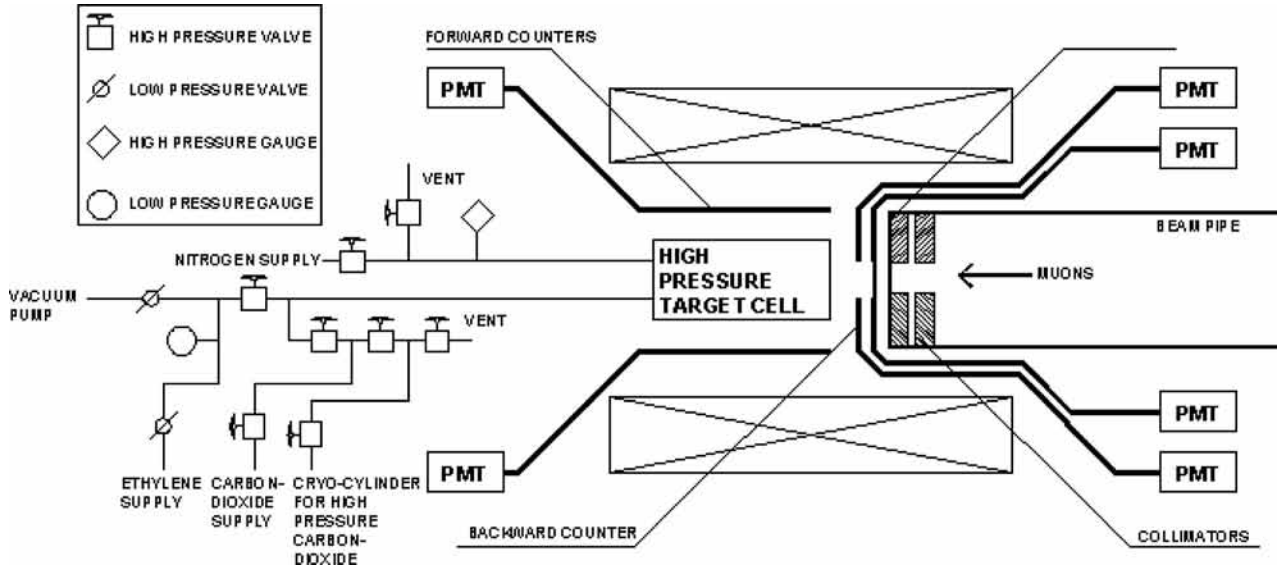

Figure 1. Schematic of the setup used for studies in this work. The two crossed-out rectangles represent the longitudinal cross section of the superconducting solenoid.

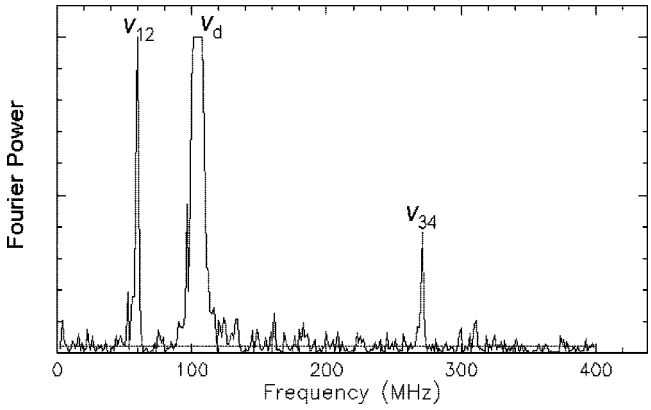

Figure 2. Transverse magnetic field spectrum of $C_2H_4Mu^{\bullet}$ at 373.15 K and 15.35 MPa in $scCO_2$ in a transverse magnetic field of 7800 G. The peaks labeled ν_{12} and ν_{34} are due to the radical and ν_d is due to diamagnetic species; the frequency ν_{12} is actually negative but the Fourier transform displayed shows only the absolute value of the frequencies.

solenoid in Figure 1), whose magnetic field was aligned along the beam direction.

CO_2 from Praxair (Research grade CO_2; 99.999%) was purified by alternate freeze/pump/thaw cycles to remove oxygen and CO prior to transfer to the pressure vessel, until any remaining dephasing of the Mu signal could be attributed to the effects of magnetic field inhomogeneity.[21] For CO_2 at least five freeze/pump/thaw cycles were done for each new load. The gradual freezing was done by inserting the lowest part of a high-pressure gas storage vessel (cryo vessel) in liquid nitrogen, and thawing was done with a heat gun. The initial concentration of O_2 was less than 2 ppm, that of CO was less than 0.1 ppm, and the total hydrocarbon content was less than 0.1 ppm. Based on the observed dephasing of the Mu signal, the total concentration of oxygen, CO, and any potential reacting hydrocarbon must be less than 1 ppb in the sample gas obtained after the series of freeze/pump/thaw cycles. The ethene from Praxair (research grade) was also purified by a series of freeze/pump/thaw cycles (at least six cycles) to remove oxygen prior to irradiation. The initial oxygen impurity of ethene was $O_2 < 1$ ppm, $CO < 1$ ppm, $CH_4 < 1$ ppm, $C_2H_2 < 1$ ppm, and $C_2H_6 < 1$ ppm. Again after the series of freeze/pump/thaw cycles the total concentration of oxygen, CO, and CH_4 must be less than 1 ppb. In the freeze/pump/thaw cycles the level of C_2H_6 would not change, but since $[C_2H_6]$ is less than 1 ppm and our solutions in CO_2 are dilute, such impurities would have negligible effects on the experimental results.

The temperature was monitored with a type K thermocouple at the center of the sample volume.

The spin polarization of the muon beam was perpendicular to the applied magnetic field for the transverse field-μSR (TF-μSR) experiments and parallel to the field for avoided level crossing-μSR (ALC-μSR) experiments,[19,20] with the positron counters positioned appropriately.

In TF-μSR the magnetic field is applied perpendicular to the spin of the muon. The precession frequency of the spin varies as a function of the strength of the magnetic field and the electronic environment, through the hyperfine interaction. At high magnetic fields where Zeeman states are sufficiently separated, only two transitions, ν_{12} and ν_{34}, are observable.[19,20] Fourier transformation of the time spectrum shows three frequency peaks, two of which correspond to the generated radical (ν_{12} and ν_{34} in Figure 2) and one to muons in a diamagnetic environment (ν_d). These frequencies can be used to determine the muon hfc, A_μ,[19,20] according to

$$\nu_{ij} = \nu_d \pm \frac{1}{2}A_\mu \tag{1}$$

However, when the free radical formation rate is not very fast compared to the rate of spin precession, the second frequency at ν_{34} lacks adequate signal-to-noise ratio due to dephasing during the reaction time, while ν_{12}, the lower frequency signal, may still be observed. This is the case for the data taken at 0.01 M ethene. The frequency peaks ν_{12} and ν_{34} are positioned symmetrically around the diamagnetic peak, and when only a strong ν_{12} is present, the hfc can be found using the following equation:[19]

$$\nu_{12} = \nu_{\mathrm{mid}} - \frac{1}{2}A_\mu \tag{2}$$

and

$$\nu_{\mathrm{mid}} = \frac{1}{2}\left[\left\{A_\mu{}^2 + (\nu_e + \nu_d)^2\right\}^{1/2} - \nu_e + \nu_d\right] \tag{3}$$

where ν_e is the electron Larmor frequency. The muon Larmor frequency, expressed in terms of the gyromagnetic ratio $\gamma/2\pi = 0.013\,553\,4$ MHz G^{-1}, is given by $\nu_\mu = \gamma_d B = g\mu eB/2m_\mu$.

Once the muon hfc is known, the proton hfc (A_p) can be obtained, from ALC-μSR measurements through the following equation:[19,20]

$$B_{\mathrm{LCR}} = \frac{1}{2}\left[\frac{A_\mu - A_p}{\gamma_\mu - \gamma_p} - \frac{A_\mu + A_p}{\gamma_e}\right] \tag{4}$$

where B_{LCR} is the magnetic field on resonance, and $\gamma_p$and γ_e are the proton and electron gyromagnetic ratios, respectively.

3. Computation

Density functional calculations on the free radicals were performed using the Gaussian 03 package of programs.[28] The geometries of the radicals were optimized with the unrestricted B3LYP functional[29] and the 6-311++G(2df,p) basis set, and the harmonic vibrational frequencies of the free radicals were calculated at the same level on the optimized structure. The isotopes were included in the calculations using the ReadIsotope option, with the mass of Mu given as 0.1140 amu.

4. Results and Discussion

Muon irradiation of solutions of ethene in $scCO_2$ in the concentration range 0.01−0.03 M at different temperatures and pressures produced signals characteristic of a muoniated radical. Figure 2 shows a Fourier transform TF-μSR spectrum in a 0.03 M solution at 373.15 K and 15.35 MPa in an applied transverse magnetic field of 7800 G. In this case, the muon hfc could be obtained using eq1.

Muon hfc's for several thermodynamic conditions are listed in Table 1. Assuming that the radical is the ethyl radical, the proton hfc's, $A_p(\alpha)$ and $A_p(\beta)$ (see Scheme 1 for proton labeling) can be obtained from ALC-μSR experiments. ALC-μSR spectra of the $C_2H_4Mu^{\bullet}$ protons for two thermodynamic conditions, 313.15 K, 8.5 MPa, and 423.15 K, 20 MPa (both at a density of 0.3 g/cm^3), were recorded over the appropriate field range.

Figure 3 shows the ALC-μSR resonances observed at 313.15 K, 8.5 MPa. The ALC-μSR resonance fields were obtained by fitting the data to Lorentzian shapes (the differential-like shapes in Figure 3 are due to the application of a small square modulation field of $\approx \pm 60$ G during the scan). Using eq 4 and

TABLE 1: Muon hfc's of $C_2H_4Mu^{\bullet}$ in $scCO_2$[a]

temperature (K)	pressure (MPa)	A_μ (MHz)
313.15(1)	8.5(4)	331(1.5)
373.15(1)	15.3(5)	330(1)
373.15(1)	15.8(1)	326(1)
373.15(1)	16.9(1)	318.2(7)
373.15(1)	18.2(1)	319.0(7)
372.95(3)	21.1(2)	322.0(1)
373.15(2)	26.3(5)	317.0(6)
423.15(1)	20.1(5)	310.9(2)

[a] Statistical uncertainties on the last digit are shown in parentheses.

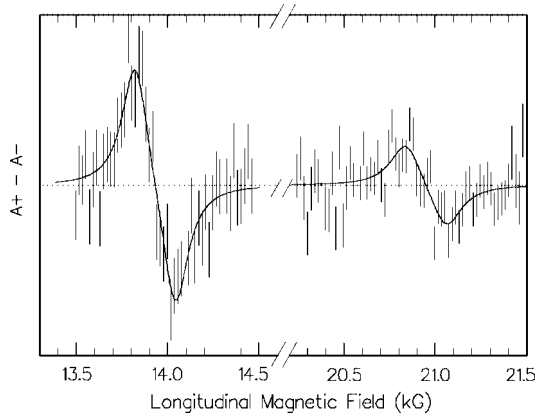

Figure 3. ALCR spectrum of $C_2H_4Mu^{\bullet}$ at resonance. Conditions: 0.01 M ethene in supercritical CO_2 at 8.5 MPa and 313.15 K. The low-field resonance corresponds to the β-proton while the high-field one corresponds to the α-proton. The solid curves represent a fit to the experimental data shown as vertical lines extending over their statistical uncertainties.

TABLE 2: ALC-μSR Resonance Positions and Corresponding hfc's[a]

temperature (K)	pressure (MPa)	β-resonance (G)	β-proton hfc (MHz)	α-resonance (G)	α-proton hfc (MHz)
313.15(1)	8.5(4)	139 303(4)	71.2(2)	20 962(7)	−59.6(2)
423.15(1)	20.1(5)	12 862(2)	70.5(2)	20 055(3)	−62.8(1)

[a] Statistical uncertainties are shown in parentheses.

the muon hfc from the TF data, the proton hyperfine coupling constants could be extracted. The data and the corresponding hfc's are presented in Table 2.

Our measured muon and proton hfc's along with previously measured hfc's in the gas and liquid phase are presented in Figure 4. In order to compare the hfc's of proton and muon, which have different gyromagnetic ratios (γ), we have referred to the reduced hfc $A = A_\mu(\gamma_p/\gamma_\mu) = A_\mu/3.1829$.

Based on previous results on the ethyl radical in the gas and liquid phase at lower temperatures and pressures,[22] as well as our theoretical calculations (see the Supporting Information), the hfc and the ALC resonance values are completely consistent with the only radical observed here as being the muoniated ethyl radical $C_2H_4Mu^{\bullet}$.

One of the results from the present study is that there is no evidence of any other radical being formed in the solutions of ethene in supercritical CO_2. If one is to use supercritical CO_2 solvent for free radical chemistry, it is important to determine whether the alkyl radical generated would react with CO_2 to form alkyl carbonyloxyl radicals.[6] This could also have implications in the use of CO_2 as a carbon source for the production of valuable chemical commodities.[6] Chateauneuf et al. proposed the possibility of the carbonyloxyl radical formation in supercritical CO_2. According to Le Chatelier's principle, the high

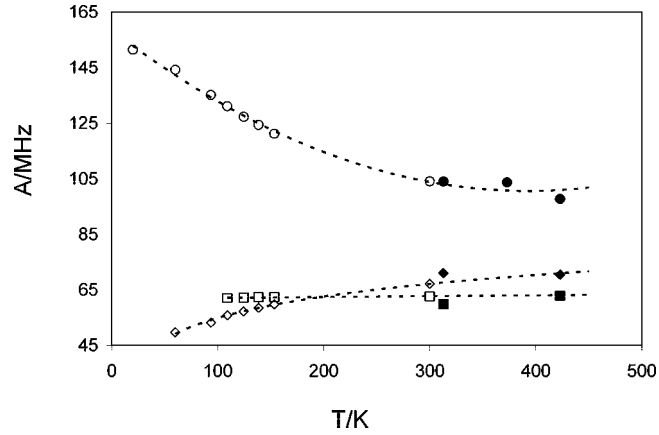

Figure 4. Temperature dependence of the reduced muon (filled circles) and β-proton (filled diamonds) and the *absolute values* of α-proton hyperfine constants (filled squares) for $C_2H_4Mu^{\bullet}$ in supercritical CO_2 at 0.30 g/cm^3, compared to the data obtained for the same radical in ethene in the liquid and gas phase from ref 22. Open symbols are data in pure ethene. The filled symbols are the data in supercritical CO_2. The dotted lines show the extrapolation to high temperature using the lower-temperature ethene data. The error bars are smaller than the size of the symbols.

TABLE 3: Free Energies and Electronic Energies for Potential Reactions between Mu and Ethene (First Row), Mu and CO_2 (Rows 2 and 3) and Ethyl and CO_2 (Rows 4 and 5) Calculated at 0 K with B3LYP DFT Method and 6-311++G(2df,p) Basis Set

radical product of the reaction	free energy of reaction (kJ mol^{-1})	electronic + thermal energy (kJ mol^{-1})
$^{\bullet}CH_2-CH_2Mu$	−134.01	−154.30
$O=C^{\bullet}O-Mu$	17.49	−2.85
$MuCO_2^{\bullet}$	57.99	37.44
$CH_2Mu-CH_2-CO_2^{\bullet}$	133.43	71.25
$CH_2Mu-CH_2-O-C^{\bullet}=O$	111.50	92.04

density of CO_2 under supercritical conditions would shift the equilibrium for the reaction of an alkyl free radical with CO_2 toward product formation.[6] Chateauneuf et al. did not observe carbonyloxyl radicals from methyl radical (which could have been generated by photochemical dissociation of alkylcolbaloximes) in supercritical CO_2.

As such, they concluded that even if the alkyl radicals react with supercritical CO_2 to produce RCO_2, the lifetime of RCO_2 is not long enough to be trapped by the hydrogen atom donor.[6] In the present experiment, we have not observed any radical other than the ethyl radical at any of the thermodynamic conditions used (the free radicals from the addition of ethyl to CO_2 would have much smaller hfc; see the Supporting Information), nor have we observed a large spin relaxation that would suggest a reaction of CO_2 with the ethyl radical. Therefore, most probably, RCO_2 does not form. To further eliminate such a possibility, we performed computational studies on the energetics of this reaction and of the formation of other radical species from Mu addition to CO_2 (see Table 3). Of different possible free radicals (see the Supporting Information), only the ethyl radical (Scheme 1) and the products of its addition to CO_2 lead to a free radical with two magnetically unequivalent protons as observed by ALC-μSR experiments. Owing to its strong C=O bonds, thermal abstraction reactions of H (Mu) are not likely.[30] Similarly the H abstraction from ethene is not likely. While the addition reaction forming HOCO (MuOCO) is energetically favorable, this reaction has a positive free energy (Table 3) and a large activation barrier.[30,31]

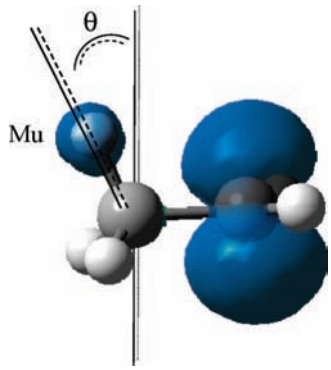

Figure 5. Schematic presentation of dihedral angle, θ, between the C−Mu bond and the plane having the C−C bond and the singly occupied p-orbital on the radical center C.

TF studies in the gas-phase ethene have suggested epithermal formation of the ethyl radical.[32] Therefore, at lower densities of CO_2, one could expect Mu* (epithermal Mu) reactions such as those with CO_2 or ethene. The reaction of H* + CO_2 from photolysis in matrix is known.[33] However, neither MuOCO nor $MuCO_2$ has been observed in pure CO_2.[21] Of course, the addition of ethene could change the environment of supercritical CO_2 as a cosolvent does.[34] On the other hand, since neither MuOCO nor $MuCO_2$ has been observed in our experiments (see the Supporting Information), we conclude that Mu is thermalized before any reaction, including the reaction with ethene, even in the lower density range of our studies. Further evidence for the thermal reaction of Mu comes from the observation that, at 0.01 M concentration of ethene and 0.3 g/mL density, the ALC-μSR signal can still be easily observed as the temperature is lowered while the TF radical amplitude becomes smaller (by almost a factor of 2 between 423.15 and 313.15 K). ALC-μSR spectra are collected in magnetic fields parallel to the spin polarization, and, therefore, are not sensitive to loss of transverse polarization. This is in contrast to the detection of the ethyl radical in ethene (in the range 0.1–1.6 MPa),[27] where the much larger (and temperature independent) TF amplitudes observed were taken as evidence for epithermal formation of the radical.[32] Therefore, our present data suggest that the ethyl radical is the outcome of *thermalized* Mu reaction with ethene.

As can be seen from the results of our calculation in Table 3, such reactions would be endoergic; therefore, our experimental data, along with our computational results, suggest that supercritical CO_2 is a chemically inert medium for the ethyl radical.

The decrease of the muon hfc with increasing temperatures (Figure 4) can be attributed to different weightings of the rotational conformers.[22–24,26,35] The temperature dependence is interpreted as due to the fact that the C−Mu bond is selectively oriented in a position close to parallel to the singly occupied p-orbital on the radical center; i.e., θ, the corresponding dihedral angle, is close to 0° (see Figure 5). The preference for Mu to occupy the $\theta = 0°$ position is seen as a result of delocalization of the singly occupied molecular orbital between the radical center C and the adjacent CH bond in the same plane, making the corresponding C−H bond weaker and longer.

At 0 K, the total energy includes only the electronic energy and the zero-point vibrational energy (ZPVE). Within the Born−Oppenheimer approximation, the electronic energies of Mu and H isotopomers are the same, and therefore, the ZPVE is the only factor that varies among different conformations at 0 K. Since the ZPVE of a C−H stretching vibration within the harmonic oscillator approximation is proportional to $(k/m)^{1/2}$,

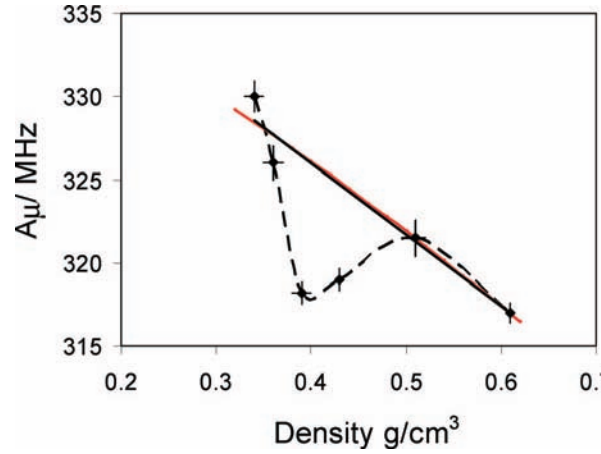

Figure 6. Density dependence of muon hyperfine constants for $C_2H_4Mu^{\bullet}$ in supercritical CO_2 at 373.15 K. The curved dashed line is to guide the eye. The solid black line represents the linear fit to the hfc's as a function of density excluding the two points around 0.4 g/cm^3 (at minimum). The solid red curve is the fit of the hfc's to the model of Vujošević et al in ref 16.

where k is the force constant and m is the mass of the hydrogen isotope, the increase in the ZPVE will be smaller for bonds with smaller force constants. Thus, the muonium atom occupies the site with the smaller force constant (i.e., the $\theta = 0°$ position). Since the free radical can exist in several rapidly interchanging conformers, assuming that the interchange rate is much larger than the difference between the associated hyperfine frequencies, a mean hfc will be observed:

$$\langle A \rangle = \sum_i P_i A_i \qquad (5)$$

where P_i is the probability of finding the ith conformer and A_i is the corresponding hfc.

Different conformational minima along the rotational potential energy surface have different ZPVEs depending on the position of Mu. The rotational conformers where Mu occupies less favorable sites have appreciable probabilities at higher temperatures. If a free radical can exist in several rapidly interchanging conformers when the interchange rate is much larger than the difference between the associated hyperfine frequencies, one measures a Boltzmann-weighted average of the hfc.[35] At higher temperatures, more rotational levels are occupied with increasing probability. The hfc's reported here fall in line with the lower temperature data obtained in the gas phase (Figure 4). This suggests that the structure, vibrational frequencies, and rotational barrier for rotation of the (muoniated) methyl group, as well as the degree of hyperconjugation, are not significantly affected in supercritical CO_2, even at pressures as large as 20 MPa at a density of 0.3 g/mL. It should be noted that previous works on ethyl radical in the gas phase and liquid phase showed no phase effect.[22,27] This lack of significant phase effect may suggest that the change in the density should not affect the hyperfine interactions in the ethyl radical. As we demonstrate below, this is *incorrect* in supercritical CO_2; however, the temperature dependence of the hfc suggests that, in the low-density regime, supercritical CO_2 behaves as an inert medium with minimum intermolecular interaction.

To further investigate the effect of supercritical CO_2 on the electronic structure of the ethyl radical, we studied the effect of the density on hfc's by varying the pressure under isothermal conditions at 373.15 K. The results are presented in Figure 6, where it is clear that the density of CO_2 significantly affects

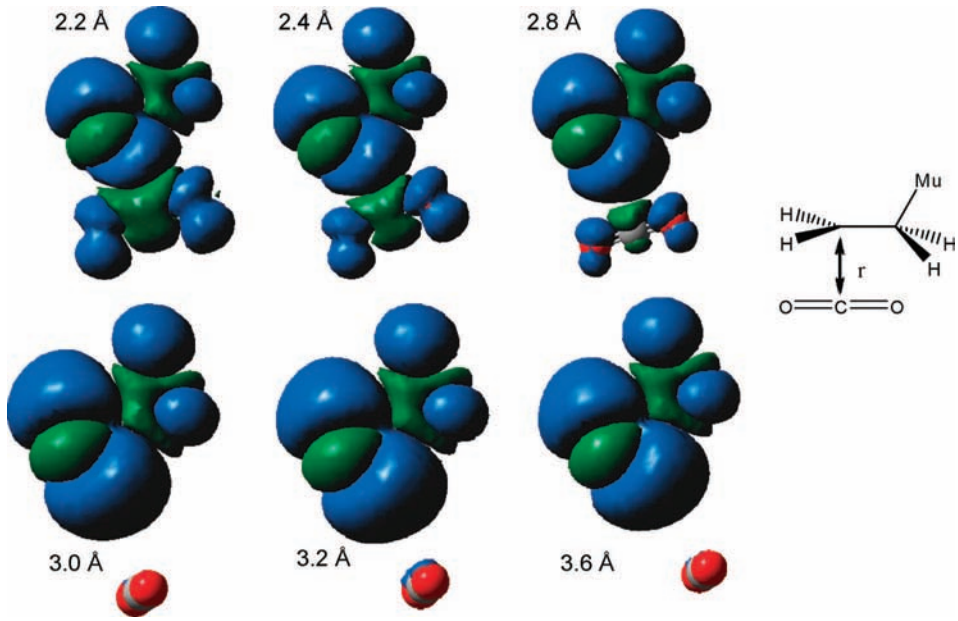

Figure 7. Spin density associated with the ethyl radical−CO_2 complex at different distances from 2.2 to 3.6 Å between CO_2 and ethyl radical. The scheme in the inset shows the definition of the distance which was varied.

the muon hyperfine coupling constant. This was not known a priori, and it is a remarkable observation. To our knowledge, there has never been any report of significant density effect on hyperfine interactions of any alkyl radical in supercritical fluids and this is the first reported case of the effect of density on hfc of a nonpersistent free radical in supercritical CO_2. The large density dependence points to the unique nature of supercritical CO_2, whereby a small change in pressure (density) can alter the electronic environment of a simple free radical. Since the temperature dependence at 0.3 g/cm^3 follows the same trend as in the gas phase, it seems likely that CO_2 molecules do not significantly affect the geometry and vibrational/rotational motions, but *the electron distribution in the ethyl radical is significantly influenced by the presence of CO_2 molecules at higher densities*.

Kauffman reported significant quadrupolar solvent−dipole solute interactions for a stable dipolar solute dissolved in CO_2 and predicted that this could be generalized to other solutes.[36] Vujošević et al. predicted that the quadrupole−dipole interactions could have significant effects on the hfc's of the free radicals.[16] Ethyl radical is polar, and can polarize the solvent cage made from CO_2 molecules by dipole−quadrupole interactions. Vujošević et al. showed that the difference of the hfc in the solvent, compared to the gas-phase values, is linearly dependent on the potential difference along the radical dipole moment in the case of the $C_6H_7^{\bullet}$ radical interacting with benzene molecules.[16] If a similar argument is used for ethyl radical, it is expected that a larger difference from the gas-phase hfc data would correlate to a larger potential difference along the ethyl radical dipole moment. This means supercritical CO_2 has significantly changed the potential difference along the ethyl radical dipole moment.

As the density increases, the hyperfine coupling decreases significantly, due to combination of two effects:

(a) The number of collisions between CO_2 molecules and ethyl radical increases. If the collision were to cause a partial transfer of unpaired electron density to CO_2 molecules, this would lead to a decrease of hfc's with density.

(b) The average distance between ethyl radical and CO_2 molecules could decrease. Such a decrease in distance means larger interactions between quadrupoles of CO_2 molecules of the solvent cage and the dipole moment of the ethyl radical.

Vujošević et al. showed that a slight decrease in the distance of a free radical (C_6H_7) and the molecules of a solvent without any dipole moment but with quadrupole moment (C_6H_6) causes significant deviation of hfc's from the gas-phase values. To investigate both effects, we performed computational studies. During the collisions, the distance between the CO_2 molecules and ethyl radical decreases. To check the effect of the distance on electron density and hyperfine coupling constants in ethyl radical, we performed DFT calculations at the levels mentioned in the Computation section. Figure 7 presents the geometry at the global minimum and unpaired spin densities, calculated at 0.0004 isodensity, at several distances in the case of ethyl radical and one CO_2 molecule (from radical center in ethyl to carbon in CO_2; see Figure 7). As the density decreases, it is clear that the relative conformation of CO_2 around ethyl radical changes with distance and the spin density is partially transferred to the CO_2 molecules, which suggests that the resulting effects of collisions are a decrease in the spin density in ethyl radical and probably a decrease in the hfc of muon in the radical.

In Figure 8, we have shown the muon hfc's at 0 K as a function of r, distance between CO_2 and ethyl (See Figure 7 for definition of r). Consistent with the result of spin densities, the data in Figure 8 suggest a decrease of the muon hfc's in the muoniated ethyl radical with a decrease of r.

The experimental data were obtained at 373 K; therefore, we have simulated the temperature dependence as a function of r. Assuming that the different rotational conformers are populated according to the Boltzmann distribution, a dependency on the temperature can be computed using a Boltzmann-weighted average of hfc's over different conformations at the energy minima along the rotational potential energy surface using eq 5 (see Figure 9). In one minimum, Mu occupies the $\theta = 0°$ position (Figure 5); in the two other minima, H occupies this position. From the data on hfc's shown in Figure 9, we can see that the general trend at 0 K (decrease of hfc with distance between CO_2 and ethyl radical) is also observed at higher temperatures, including at 373 K, the experimental temperature.

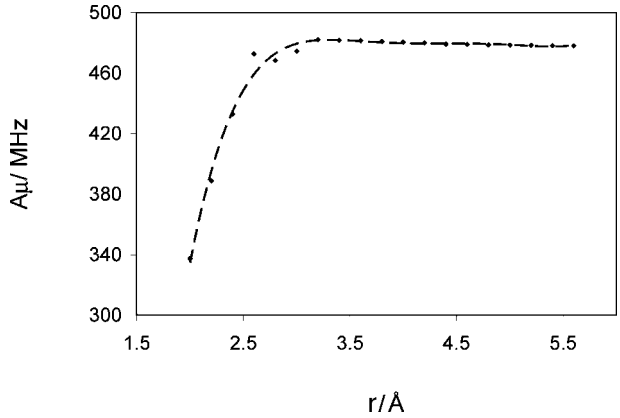

Figure 8. Calculated muon hfc's as a function of separation between the ethyl radical and CO_2.

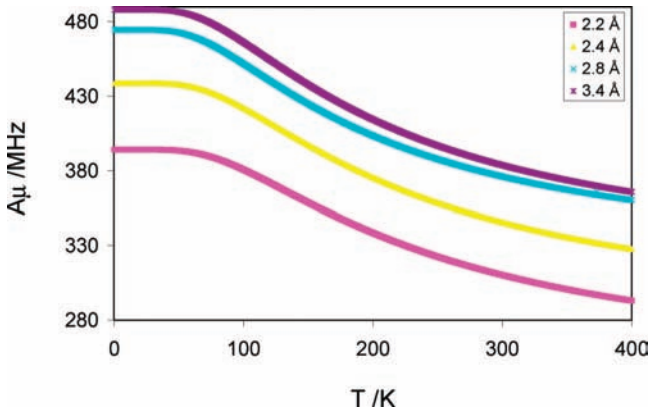

Figure 9. Computed temperature dependence of muon hfc's as a function of distance between the central carbon in carbon dioxide and the radical center of the ethyl radical.

Another result from the data in Figure 6 is a deviation from a smooth density dependence of the hfc. It is clear that the overall density dependence is not linear. The strong change in the curvature at densities slightly lower than the solvent's critical density, as observed here, could be due to "clustering" of CO_2 molecules around the ethyl radical.[36–40] Alternatively, it might be a result of the balance between repulsive and attractive interactions between the solute and solvent molecules.[39,40] The clustering in supercritical CO_2 can be interpreted as a different local density around ethyl radical than the bulk density. Based on the observed trend in Figure 6, we can deduce an increase in the clustering around 0.4 g/cm^3 followed by breaking of the clusters at larger densities up to 0.5 g/cm^3. To gain an estimate of the local density, we can remove the two points closest to the minimum (around 0.4 g/cm^3 in Figure 6), find the hfc's as a function of density, and then use the obtained equation to predict the local density at the minimum. Excluding the two points close to the minimum, a linear fit to the experimental data is reasonable within the errors of the experimental data in Figure 6. Using the linear equation, the local density at the minimum around 0.40 g/cm^3 (the bulk density) is 0.58 g/cm^3. Vujošević et al. used a model in which the electric dipole of a free radical causes local ordering of solvent molecules, thus producing an external electric field, polarizing the free radical. Using this model, they showed that the difference between the hfc in the solvent and the gas-phase values increases according to $[Q]^{4/3}$, where [Q] is the concentration of quadrupole moments in solution.[16] This model applies to a solvent that does not have a dipole moment but which does have a quadrupole moment, such as $scCO_2$.[16] The red curve in Figure 6 is the fit of the hfc's to their model (excluding the two points around minimum). Within our experimental errors, there is little difference in the agreement of the fit to their model with the simple linear fit of hfc's to density. Using the model of Vujošević et al., the local density would be 0.63 g/cm^3. Therefore, our estimate for the local density around ethyl radical at the bulk density of 0.40 g/cm^3 is 0.6 g/cm^3, which means that the local density around ethyl radical is almost 1.5 times larger than the bulk density. Since there is minimal difference between the predictions of the simple linear fit and the model of Vujošević et al. (Figure 6), we have used the linear density dependence to estimate the average distance between the ethyl radical and the CO_2 molecules forming the solvent cage.

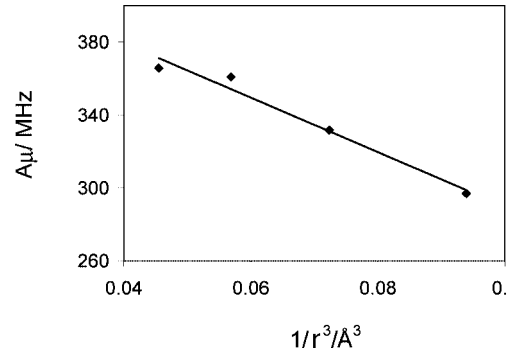

Figure 10. Computed muon hfc's at 373.15 K as a function of $1/r^3$, where r is the distance between CO_2 molecule and ethyl radical. Diamonds are the results of the DFT calculation. The line is a linear fit according to the equation $A = -1494.8/r^3 + 439.2$.

Assuming an average spherical CO_2 solvent cage around ethyl radical, a linear density dependence of hfc's in the muoniated ethyl radicals, as explained above, could be due to changes in the average distance between the ethyl radical and the surrounding CO_2 molecules. The average distance between the ethyl radical and the surrounding CO_2 molecules is not known experimentally, but we can assume it is proportional to the inverse cube root of the density ($\rho_{CO_2}^{-1/3}$). Therefore, the linear density dependence of hfc's (as long as there is no density inhomogeneity) could indicate an inverse cubic relationship between hfc's and the average distance between CO_2 molecules of the solvent cage and ethyl radical. In Figure 10, we plotted the theoretical predictions of hfc's as a function of inverse of r^3, where r is the distance between CO_2 and ethyl radical (Figure 7) at 373.15 K. It is evident that the linear fit is reasonable with a square of the Pearson product moment correlation coefficient of 0.98. In the presence of density inhomogeneity, as stated earlier, the local density is larger around the ethyl radical when compared to the bulk density. From the above analysis of the dependence of the hfc on the distance between ethyl radical and CO_2 molecules of the solvent cage, we can estimate an upper limit of 1.2 times for the decrease in average CO_2−ethyl distance at ~0.4 g/cm^3 compared to the distance that would have been expected if there was no inhomogeneity in the density.

Although a more quantitative understanding of the extent of enhanced solvent density around the solute and detailed analysis of quadrupolar solvent−dipole solute interactions and collisional effects on hfc's of ethyl radical in near-critical CO_2 should incorporate the use of molecular dynamics computer simulations,[39,40] the observed density dependence of the hfc's of ethyl radical certainly suggests that CO_2 is not just a "heavy gas." At higher densities, it could be used as a solvent to tune the reactivity of free radicals, while the temperature dependence at

lower densities demonstrates that the electronic structure of free radicals (and hence their reactivity) is almost intact and independent of CO_2 molecules in the low-density regime.

5. Conclusion

In summary, the following new information has been obtained from our studies:

(1) Muonium can be used (in lieu of H atom) for generation of transient radicals in $scCO_2$.

(2) Even at low concentrations of ethene in $scCO_2$, the muonium (and by analogy H) atom adds to ethene and the resulting ethyl radical (and most probably any alkyl radical) is not reactive toward molecules of CO_2 in $scCO_2$.

(3) Addition to ethene to form an alkyl radical in $scCO_2$ is enhanced compared to normal liquids.

(4) CO_2 molecules have significant intermolecular interactions with the ethyl radical at higher densities, which causes unexpected density dependency of hfc's.

(5) There is partial transfer of unpaired electron density from alkyl radical into CO_2 molecules of the solvent cage at higher densities due to combination of two effects: (a) When the density increases, the number of collisions between CO_2 molecules and ethyl radical also increases. (b) When the density increases, the average distance between ethyl radical and CO_2 molecules decrease. Such a decrease in distance means larger interactions between quadrupoles of CO_2 molecules of the solvent cage and the dipole moment of the ethyl radical. Since the reactivity of free radicals depends on the distribution of the unpaired electron density within them, we can conclude that it is possible to tune the reactivity of free radicals by making a small adjustment to the density (pressure) in supercritical CO_2. This could have implications on free radical polymerization in $scCO_2$.

(6) The local density around ethyl radical is almost 1.5 times larger than the bulk density at 0.4 g/cm^3.

When compared with results of similar studies in the liquid phase and the gas phase, studies of neutral and nonpersistent radicals in $scCO_2$, such as the studies reported here, can provide valuable information on free radical reactions in supercritical CO_2, for which there is limited microscopic knowledge. The present paper highlights the use of μSR spectroscopy as a tool to probe free radical chemistry in $scCO_2$ and provide such microscopic information.

Acknowledgment. This work was financially supported partially by the Natural Sciences and Engineering Research Council of Canada to K.G. and, through TRIUMF, by the National Research Council of Canada. It was also financially supported partially by the Mount Allison Majorie Young Bell Faculty fund and The New Brunswick Innovation Foundation. We thank Prof. P. W. Percival from Simon Fraser University for allowing us to use their high-pressure vessel and ALCR system. We thank Chris Alcorn for assistance with data taking and the staff of the TRIUMF Centre for Molecular and Materials Science for technical support. The Mount Allison Cluster for Advanced Research (TORCH) was used for all quantum calculations.

Supporting Information Available: Complete ref 28. Details of computations. A TF spectra of 0.01 M ethene in $scCO_2$. This information is available free of charge via the Internet at http://pubs.acs.org.

References and Notes

(1) Rayner, C. M. *Org. Process Res. Dev.* **2007**, *11*, 121–132.
(2) *Chemical Synthesis Using Supercritical Fluids*; Jessop, P. G., Leitner, W. Z., Eds.; Wiley-VCH: Weinheim, 1999.
(3) Charpentier, P. A.; Xu, W. Z.; Li, X. *Green Chem.* **2007**, *9*, 768–776.
(4) DeSimone, J. M. *Science (Washington, D.C.)* **2002**, *297*, 799–803.
(5) Banister, J. A.; Cooper, A. I.; Howdle, S. M.; Jobling, M.; Poliakoff, M. *Organometallics* **1996**, *15*, 1804–1812.
(6) Chateauneuf, J. E.; Zhang, J.; Foote, J.; Brink, J.; Perkovic, M. W. *Adv. Environ. Res.* **2002**, *6*, 487–493.
(7) Jobling, M.; Howdle, S. M.; Healy, M. A.; Poliakoff, M. *Chem. Commun.* **1990**, *18*, 1287–1290.
(8) Pacut, R.; Grimm, M. L.; Krausb, G. A.; Tanko, J. M. *Tetrahedron Lett.* **2001**, *42*, 1415–1418.
(9) Adam, W.; Diedering, M.; Trofimov, A. V. *Chem. Phys. Lett.* **2001**, *350*, 453–458.
(10) Beuermann, S.; Buback, M.; Gadermann, M.; Jurgens, M.; Saggu, D. P. *J. Supercrit. Fluids* **2006**, *39*, 246–252.
(11) Batchelor, S. N.; Henningsen, B.; Fischer, H. *J. Phys. Chem. A* **1997**, *101*, 2969–2972.
(12) Forbes, M. D. E.; Yashiro, H. *Macromolecules* **2007**, *40*, 1460–1465.
(13) Grimm, C.; Kandratsenka, A.; Wagener, P.; Zerbs, J.; Schroeder, J. *J. Phys. Chem. A* **2006**, *110*, 3320–3329.
(14) Luther, K.; Oum, K.; Sekiguchi, K.; Troe, J. *Phys. Chem. Chem. Phys.* **2004**, *6*, 4133–4141.
(15) Shkrob, I. A.; Sauer, M. C.; Jonah, C. D.; Takahashi, K. *J. Phys. Chem. A* **2002**, *106*, 11855–11870.
(16) Vujošević, D.; Dilger, H.; McKenzie, I.; Martyniak, A.; Scheuermann, R.; Roduner, E. *J. Phys. Chem. A* **2007**, *111*, 199–208.
(17) Avdievich, N. I.; Dukes, K. E.; Forbes, M. D. E.; DeSimone, J. M. *J. Phys. Chem. A* **1997**, *101*, 617–621.
(18) Forbes, M. D. E.; Dukes, K. E.; Avdievich, N. I.; Harbron, E. J.; DeSimone, J. M. *J. Phys. Chem. A* **2006**, *110*, 1767–1774.
(19) Cox, S. F. J. *J. Phys. C* **1987**, *20*, 3187–3319.
(20) Roduner, E. *Chem. Soc. Rev.* **1993**, *12*, 337–346.
(21) Ghandi, K.; Bridges, M. D.; Arseneau, D. J.; Fleming, D. G. *J. Phys. Chem. A* **2004**, *108*, 11613–11625.
(22) Percival, P. W.; Brodovitch, J. C.; Leung, S. K.; Yu, D.; Kiefl, R. F.; Garner, D. M.; Arseneau, D. J.; Fleming, D. G.; Gonzalez, A.; Kempton, J. R.; Senba, M.; Venkateswaran, K.; Cox, S. F. J. *Chem. Phys. Lett.* **1989**, *163*, 241–245.
(23) Ramos, M. J.; McKenna, D.; Webster, B. C.; Roduner, E. *J. Chem. Soc., Faraday Trans.* **1984**, *80*, 255–265.
(24) Ramos, M. J.; McKenna, D.; Webster, B. C.; Roduner, E. *J. Chem. Soc., Faraday Trans.* **1984**, *80*, 267–274.
(25) Roduner, E.; Strub, W.; Burkhard, P.; Hochmann, J.; Percival, P. W.; Fischer, H.; Ramos, M.; Webster, B. C. *Chem. Phys.* **1982**, *67*, 275–285.
(26) Webster, B.; Buttar, D. *J. Chem. Soc., Faraday Trans.* **1996**, *92*, 2331–2334.
(27) Fleming, D. G.; Pan, J. J; Senba, M.; Arseneau, D. J.; Kiefl, R. F.; Shelly, M. Y.; Cox, S. F.J.; Percival, P. W.; Brodovitch, J. C. *J. Chem. Phys.* **1996**, *17*, 7517–7535.
(28) Frisch, M. J.; et al. *Gaussian 03*, revision B.04; Gaussian, Inc.: Pittsburgh, PA, 2003. For complete reference, see Supporting Information.
(29) Becke, A. D. *J. Chem. Phys.* **1993**, *98*, 1372–1377.
(30) Duncan, T. V.; Miller, C. E. *J. Chem. Phys.* **2000**, *113*, 5138–5140.
(31) Troya, D.; Lakin, M. J.; Schatz, G. C.; Harding, L. B.; Gonzalez, M. *J. Phys. Chem. B* **2002**, *106*, 8148–8160.
(32) Percival, P. W.; Brodovitch, J. C.; Arseneau, D. J.; Senba, M.; Fleming, D. G. *Physica B* **2003**, *326*, 72–75.
(33) Scherer, N. F.; Sipes, C.; Bernstein, R. B.; Zewail, A. H. *J. Chem. Phys.* **1990**, *92*, 5239–5259.
(34) Jessop, P. G.; Ikariya, T.; Noyori, R. *Chem. Rev.* **1995**, *95*, 259–272.
(35) Ghandi, K.; Zahariev, F. E.; Wang, Y. A. *J. Phys. Chem. A* **2005**, *109*, 7242–7250.
(36) Kauffman, J. F. *J. Phys. Chem. A* **2001**, *105*, 3433–3442.
(37) Bulgarevich, D. S.; Sako, T.; Sugeta, T.; Otake, K.; Takebayashi, Y.; Kamizawa, C.; Horikawa, Y.; Kato, M. *Ind. Eng. Chem. Res.* **2002**, *41*, 2074–2081.
(38) Ingrosso, F.; Ladanyi, B. M. *J. Phys. Chem. B* **2006**, *110*, 10120–10129.
(39) Tucker, S. C. *Chem. Rev.* **1999**, *99*, 391–418.
(40) Zhou, S. *Commun. Theor. Phys.* **2005**, *44*, 365–370.

JP801023V